Annual Report

Electrooptical Devices

30 September 1986

Lincoln Laboratory

MASSACHUSETTS INSTITUTE OF TECHNOLOGY

LEXINGTON, MASSACHUSETTS

ADA193446

MASSACHUSETTS INSTITUTE OF TECHNOLOGY
LINCOLN LABORATORY

ELECTROOPTICAL DEVICES

ANNUAL REPORT
TO THE
ROME AIR DEVELOPMENT CENTER

1 OCTOBER 1985 — 30 SEPTEMBER 1986

ISSUED 23 FEBRUARY 1988

LEXINGTON   MASSACHUSETTS

ABSTRACT

This report covers work carried out with the support of the Rome Air Development Center during the period 1 October 1985 through 30 September 1986.

The small-signal frequency response of small-contact mass-transported buried-heterostructure lasers with minimal parasitic contact pad capacitance has been measured. Initial results show that the highest relaxation frequency of 5 GHz is obtained in long lasers with high optical power.

GaInAsP/InP buried-heterostructure lasers fabricated on p-InP substrates offer considerable advantages in terms of reduced series resistance because of the large-area p-contact. A simple formula has been derived that permits an accurate calculation of the spreading resistance in the p-InP.

TABLE OF CONTENTS

LIST OF ILLUSTRATIONS

ELECTROOPTICAL DEVICES

I. HIGH-FREQUENCY RESPONSE OF SMALL-CONTACT MASS-TRANSPORTED INJECTION LASERS

The small-signal high-frequency performance of diode lasers is of interest for the distribution of microwave signals over optical fibers. The response of 1.3-μm lasers is often limited by a parasitic contact pad capacitance.[1] This capacitance is formed in most laser structures by the contact pad metallization and a thin electrical insulator which overlaps the substrate material in areas outside of the actual laser stripe. The frequency response of the lasers was shown to improve as this parasitic capacitance was reduced.[1] We report initial results taken on small-contact mass-transported lasers in which the area of the contact is limited to the laser mesa and the parasitic pad capacitance is eliminated.

The lasers were fabricated using the mass-transport process as described previously.[2] Figure I-1 illustrates a cross-sectional view of the mass-transported laser. The GaInAsP active region was 2 μm wide and 0.15 μm thick. On each side of the active region were 3.5-μm-wide regions of mass-transported InP, which formed the buried heterostructure. Contact metallization was photolithographically confined to a 4-μm-wide stripe above the 6-μm laser mesa, as shown in Figure I-1. The lasers were In-soldered in a microstripline package with the stripe side up. In-coated Au ribbons were used to connect the microstripline to the contact stripe.

CONTACT PAD

p InP 9×10^{17}

GaInAsP

n InP 2×10^{18}

OXIDE
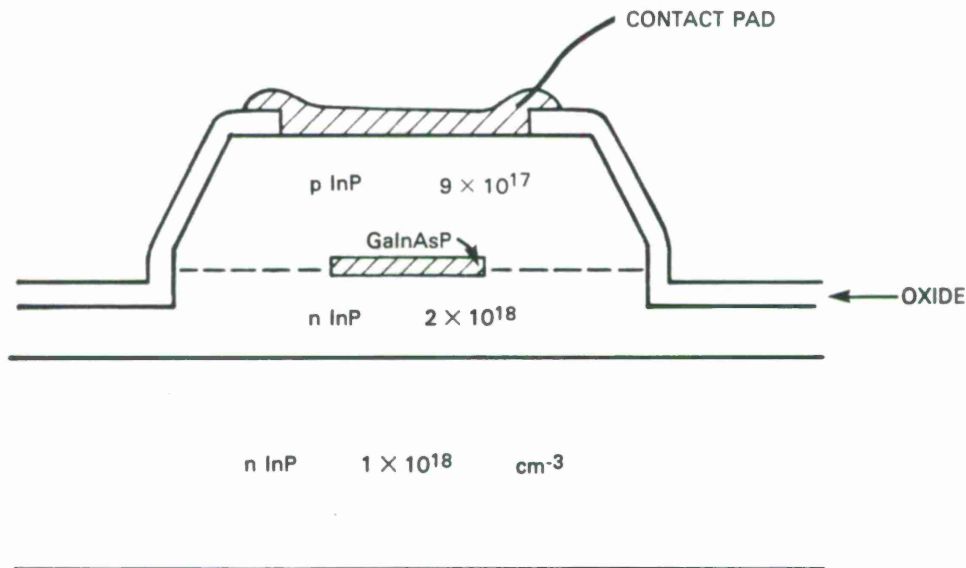
n InP 1×10^{18} cm^{-3}

Figure I-1.   Schematic cross section of small contact mass-transported diode laser. Contact is confined to top of mesa to eliminate parasitic contact pad capacitance.

1

The microwave impedance of the diode is primarily capacitive at zero bias. With forward bias, the capacitance is shorted as the diode begins to conduct and the impedance of the laser is 10 Ω up to a frequency of 7 GHz, above which lead inductance (about 0.25 nH) begins to dominate the impedance. The electrical impedance does not change with current once the diode conducts.

Frequency response measurements were made using a network analyzer with a reflection-transmission test set. The laser was connected to the output of the test set and an InGaAs detector, with a 3-dB rolloff frequency of 8 GHz, was connected to the input. The laser emission was collected with a 0.6-NA lens and focused onto the detector with a 0.5-NA lens. A wideband bias network was placed between the reflection-transmission test set and the laser without impedance matching. RF insertion loss between the input to the laser and the detector output was measured over the 0.1 to 8 GHz range using the leveled output of a sweep oscillator to drive the laser.

Figure I-2(a) through (c) shows frequency response of a 400-μm-long device for different values of dc bias current. Pronounced response peaks associated with the laser relaxation oscillation frequency are evident; they are not observed for lasers with large parasitic capacitance. The amplitude of this peak increases with increasing current, peaks at about 40 mA, and decreases with higher currents. The ratio of the power at the resonant frequency to the power at low frequencies is shown as a function of the square root of the dc optical power in Figure I-3. With low parasitic capacitance, the response is enhanced by as much as 10 dB at this resonant frequency.

The resonant frequency increases with dc bias current and the resonant peak broadens considerably. At 30 mA, just above the 25-mA threshold current, the resonance occurs at 1.4 GHz. At 90 mA the peak occurs at about 5 GHz and the response is 3 dB down from the low-frequency value at about 6 GHz. This 3-dB rolloff frequency is plotted as a function of the square root of the dc optical power in Figure I-3 and shows an approximate linear dependence.

At low frequencies (100 MHz) the total microwave insertion loss, from the input of the laser bias network to the detector output, was about 23 dB and this low-frequency insertion loss was independent of dc bias from just above the 25-mA threshold current to about 50 mA. At higher dc biases the efficiency of the laser decreases as a result of current leakage around the active layer and heating.

Initial results on these lasers indicate that longer lasers have better high-frequency performance because of higher optical power output. Measurements of a 150-μm laser show a maximum relaxation oscillation frequency of only 3.3 GHz. The output power of this 150-μm laser began to saturate near 2.5 mW, whereas the 400-μm laser did not saturate up to 8 mW. At equivalent output power, the shorter laser did have a higher relaxation oscillation frequency, as expected.

2
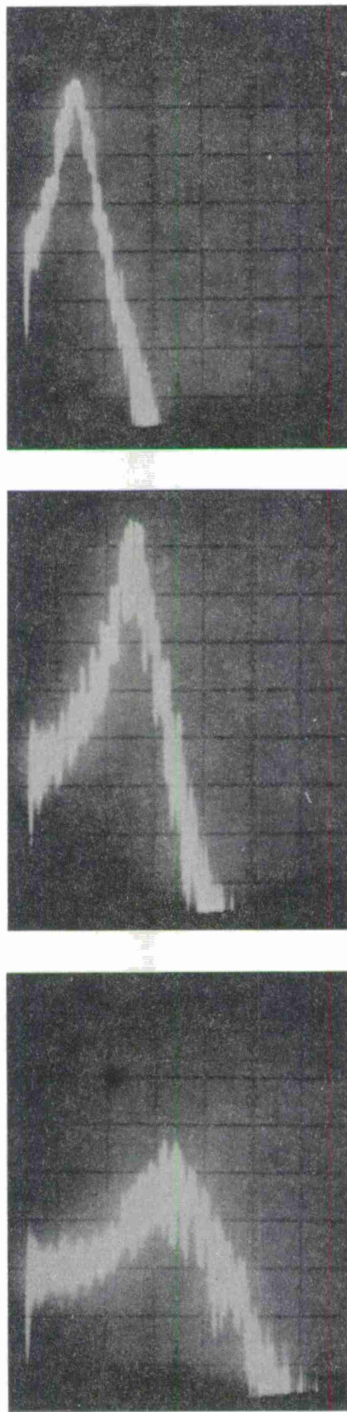
Figure 1-2.   Small-signal frequency response of a 400-μm-long laser for different DC injection current levels. The laser threshold of this device is 25 mA.
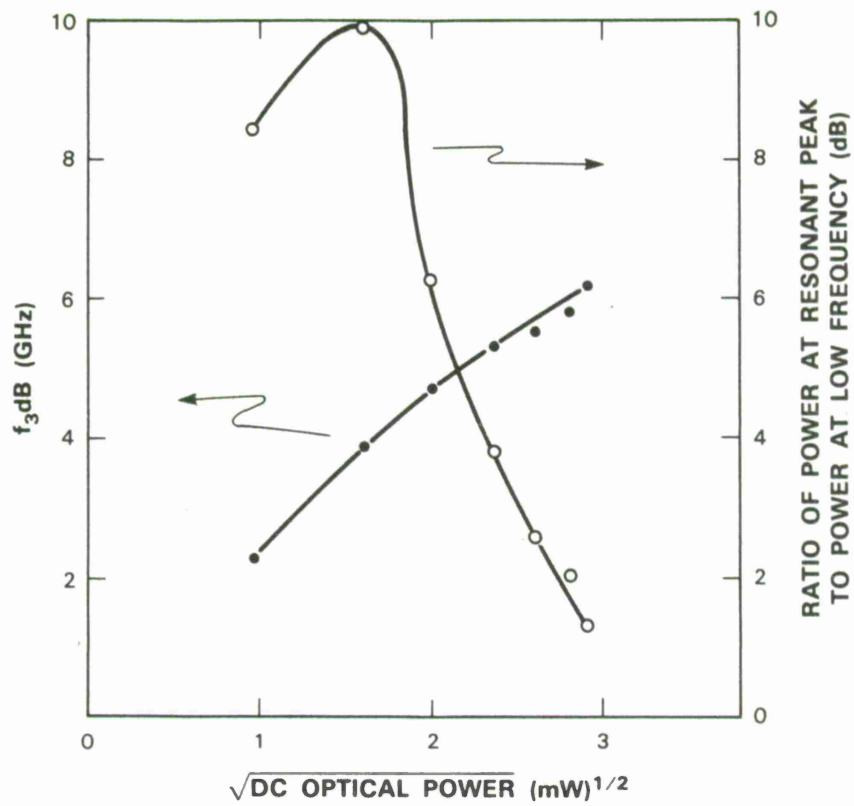
Figure I-3. Dependence of resonant peak amplitude and frequency response on DC optical power for the 400-μm laser used in Figure I-2.

Comparisons of our results with other 1.3-μm lasers show that our relaxation frequencies are similar to those seen in other buried-heterostructure lasers[1] and higher than those reported for ridge waveguide[1] and DC-PBH[3] structures. However, a 12.5-GHz relaxation oscillation frequency has been reported[4] for short-cavity vapor-phase-regrown lasers operated on a pulsed basis. Compared to the small-contact mass-transported lasers reported here, the vapor-phase regrown lasers were twice as wide and twice as thick, and had twice the doping level in the InP cap and over three times the output power per unit length. However, transverse and lateral mode quality tend to be compromised in lasers with thick and wide active regions. We are investigating means to increase the high-frequency performance of buried-heterostructure lasers while preserving lowest order mode quality.

D.Z. Tsang
Z-L. Liau

II. SERIES RESISTANCE IN GaInAsP/InP BURIED-HETEROSTRUCTURE LASERS FABRICATED ON p-TYPE SUBSTRATES

Recent development[5-7] of GaInAsP/InP buried-heterostructure diode lasers using p-InP substrates offers considerable advantages due to the large-area p contact, since the p contact is difficult to fabricate and has high specific contact resistance. In these devices, the total electrical resistance likely will be dominated by the spreading resistance in the p-InP, which has considerably higher resistivity than n-InP. In this work, the spreading resistance has been analyzed, and a simple formula has been derived that permits an accurate calculation.

The electrical current flow in the substrate of a p-InP substrate BH laser is illustrated in Figure II-1 for a laser with a 100 μm $\times$ 100 μm substrate cross section contacted at the bottom surface. In forward bias, current starts from the large-area p contact and flows into the narrow GaInAsP active layer (seen as a 2-μm-wide segment). The voltage distribution for this device geometry can be analyzed conveniently by using conformal mapping[8] from the simple case of current flowing from all directions into a slit. The latter is shown in Figure II-2(a), where the equipotentials in the z plane (z = x + iy) are confocal ellipses given by

$$\frac{x^2}{\cosh^2 \Phi} + \frac{y^2}{\sinh^2 \Phi} = 1 \quad , \tag{1}$$

where Φ is the potential. The equipotential contours become nearly circular for $\Phi \geqslant 2$. In order to determine the equipotentials for our device geometry shown in Figure II-1, we map the upper z plane into a strip in the upper w plane (w = u + iv) as shown in Figure II-2(b) using the coordinate transformation[8]

$$z = \frac{\sin \dfrac{\pi w}{2s}}{\sin \dfrac{\pi W}{2s}} \quad , \tag{2}$$

where W and s are the half widths of the active region and p substrate, respectively. By combining Equations (1) and (2), the potential $\Phi(u,v)$ is obtained, which then is converted into the voltage distribution $V(u,v)$ by[2]

$$V(u,v) = \frac{\rho I}{\pi L} \Phi(u,v) + V_Q \quad , \tag{3}$$

where ρ is the resistivity of the p-InP, I is the current, L is the device length, and V_Q is the junction voltage at the quaternary active region. (V_Q = 0.98 V when the device is lasing.[2]) Note in Figure II-2(b), that when $v \gtrsim s$, the equipotentials approach horizontal lines, and one of them will closely approximate the p contact, as shown in Figure II-1.

Figure II-1. Calculated current and voltage distributions in a p-substrate GaInAsP/InP buried-heterostructure laser. The solid and dashed curves are the equipotentials and streamlines, respectively. The equipotentials are shown in voltage increments of 0.1 V. The junction voltage at the GaInAsP active region is 0.98 V.

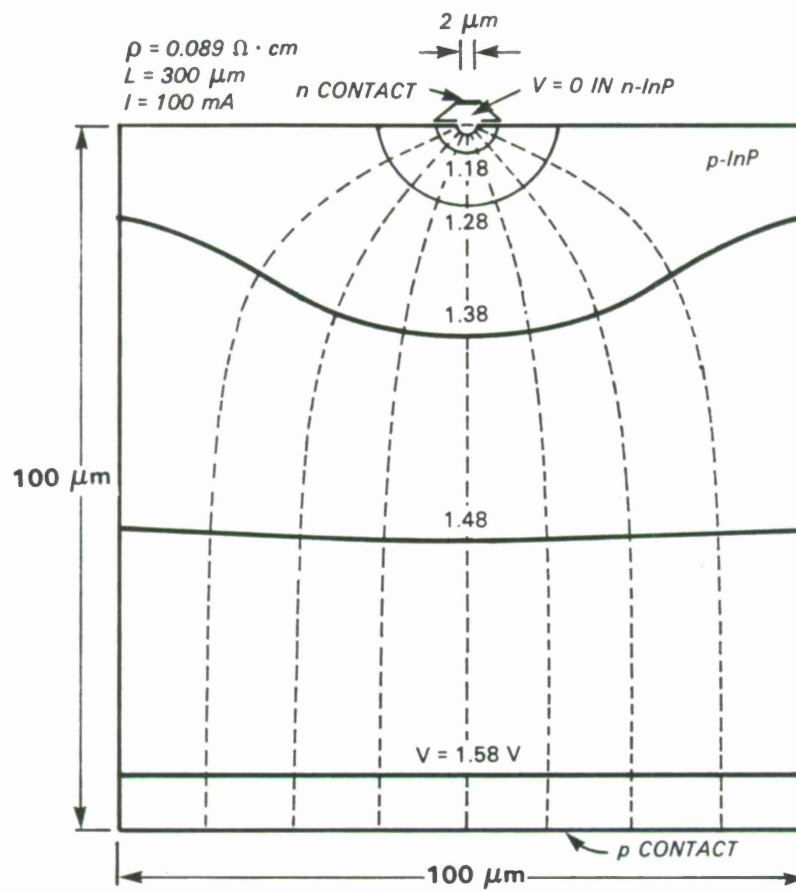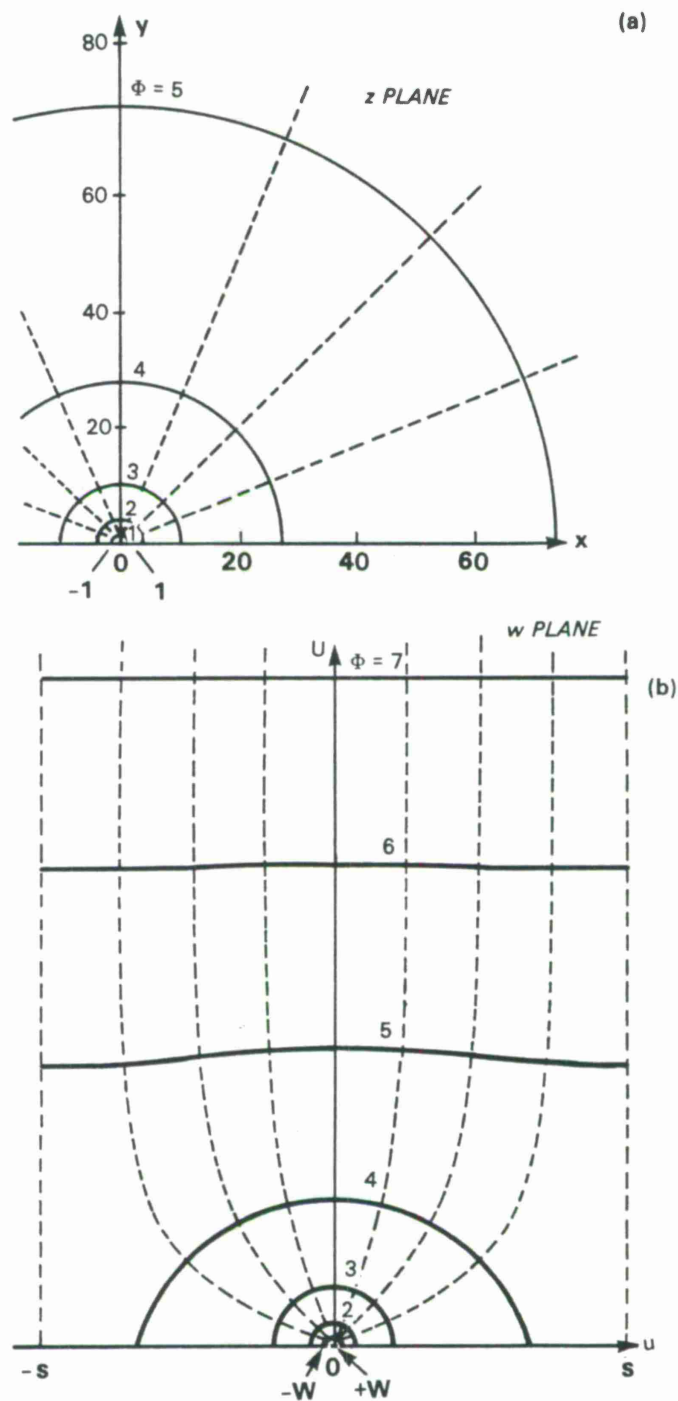*Figure II-2. The conformal mapping used to calculate the current and voltage distributions in the p-substrate buried-heterostructure laser. The solid and dashed curves are the equipotentials and streamlines, respectively. Part (a) shows the simple case of current flowing (uniformly from all directions at infinity) into a slit that is maintained at a constant potential of $\phi = 0$.*

9

To calculate the spreading resistance, only the voltage difference between the p contact and the quaternary active region needs to be evaluated. This can be done easily by considering only the transformation [Equation (2)] along the imaginary axes and by noting that $\Phi = \sinh^{-1} y$ when $x = 0$. Thus, the spreading resistance is given by

$$R = \frac{\rho}{\pi L} \sinh^{-1} \frac{\sinh \dfrac{\pi v}{2s}}{\sin \dfrac{\pi W}{2s}} \tag{4}$$

[Note that $\sinh^{-1} y$ can be conveniently expressed as $\ln (y + \sqrt{y^2 + 1})$.] Equation (4) correctly reduces to $R = \rho v / 2sL$ when $W = s$.

Equation (4) allows for a direct computation of the spreading resistance R from the device geometry and the resistivity. Figure II-3 shows that R varies slowly with 2s until $2s \lesssim v$. For typical discrete devices, $2s \simeq 200~\mu m$ and spreading resistances of 5 to 6 Ω are obtained from Figure II-3 for active region widths of 1 to 3 μm and for $\rho = 0.089~\Omega$ cm (corresponding to a hole concentration of 1×10^{18} cm^{-3} with a hole mobility of 70 cm^2/V s). Our recent experimental values of the total device resistances were $\gtrsim 10~\Omega$, indicating that perhaps the contact resistances were not negligible. It is worth noting that with minor modifications Equation (4) also can be used to calculate the thermal resistance, provided that the device is mounted junction-side-up on a heatsink and that all the heat is generated near the active region.

In conclusion, a simple formula has been derived that permits an accurate calculation of the spreading resistance in p-substrate buried-heterostructure lasers. It is highly valuable in the device design and in minimizing the series resistance.

Z-L. Liau
J.N. Walpole
D.Z. Tsang

$\rho = 0.089\ \Omega \cdot cm$
$\upsilon = 100\ \mu m$
$L = 300\ \mu m$

$$R = \frac{\rho}{\pi L}\ \sinh^{-1}\left(\frac{\sinh\dfrac{\pi\upsilon}{2s}}{\sin\dfrac{\pi W}{2s}}\right)$$
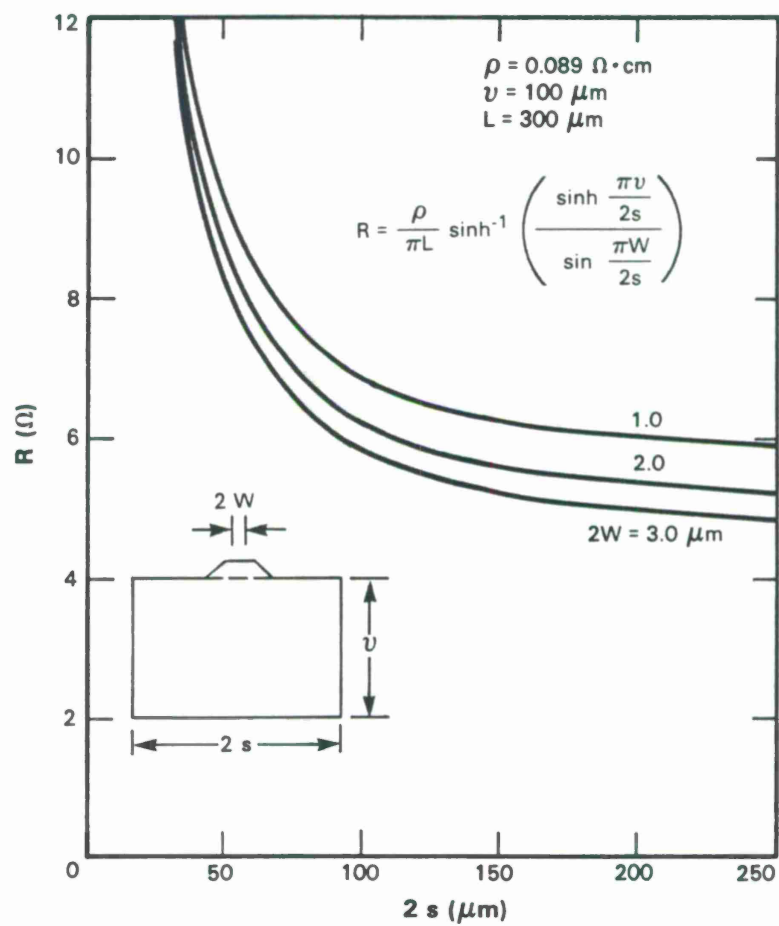
Figure II-3. Calculated spreading resistance for the p-substrate, buried-heterostructure laser as a function of the device geometry.

11

REFERENCES

1. R.S. Tucker and I.P. Kaminow, J. Lightwave Technol. **LT-2**, 385 (1984).

2. Z.L. Liau, J.N. Walpole, and D.Z. Tsang, IEEE J. Quantum Electron. **QE-20**, 855 (1984).

3. I. Mito, M. Kitamura, M. Yamaguchi, K. Kobayashi, and I. Takano, Electron. Lett. **20**, 261 (1984).

4. C.B. Su, V. Lanzisera, W. Powazinik, E. Meland, R. Olshansky, and R.B. Lauer, Appl. Phys. Lett. **46**, 344 (1985).

5. Y. Noguchi, Y. Suzuki, T. Matsuoka, and H. Nagai, Electron. Lett. **20**, 769 (1984).

6. Y. Nakano and Y. Noguchi, IEEE J. Quantum Electron. **QE-21**, 452 (1985).

7. D.C. Flanders, personal communication.

8. See, for example W.R. Smythe, *Static and Dynamic Electricity*, 3rd ed. (McGraw-Hill, New York, 1968) Chpt. 4.

REPORT DOCUMENTATION PAGE

1a. REPORT SECURITY CLASSIFICATION Unclassified		1b. RESTRICTIVE MARKINGS			
2a. SECURITY CLASSIFICATION AUTHORITY		3. DISTRIBUTION/AVAILABILITY OF REPORT Approved for public release; distribution unlimited.			
2b. DECLASSIFICATION/DOWNGRADING SCHEDULE					
4. PERFORMING ORGANIZATION REPORT NUMBER(S)		5. MONITORING ORGANIZATION REPORT NUMBER(S) ESD-TR-87-055			
6a. NAME OF PERFORMING ORGANIZATION Lincoln Laboratory, MIT	6b. OFFICE SYMBOL (If applicable)	7a. NAME OF MONITORING ORGANIZATION Electronic Systems Division			
6c. ADDRESS (City, State, and Zip Code) P.O. Box 73 Lexington, MA 02173-0073		7b. ADDRESS (City, State, and Zip Code) Hanscom AFB, MA 01731			
8a. NAME OF FUNDING/SPONSORING ORGANIZATION Rome Air Development Center	8b. OFFICE SYMBOL (If applicable) RADC/ESMS	9. PROCUREMENT INSTRUMENT IDENTIFICATION NUMBER F19628-85-C-0002			
8c. ADDRESS (City, State, and Zip Code) Griffiss AFB New York, NY 13440		10. SOURCE OF FUNDING NUMBERS			

		PROGRAM ELEMENT NO. 62702F, 61102F	PROJECT NO. 85	TASK NO.	WORK UNIT ACCESSION NO.

11. TITLE (Include Security Classification)

Electrooptical Devices

12. PERSONAL AUTHOR(S)
Tsang, Dean Z. and Williamson, Richard C.

13a. TYPE OF REPORT Annual Report	13b. TIME COVERED FROM 10/1/85 TO 9/30/86	14. DATE OF REPORT (Year, Month, Day) 1986, September, 30	15. PAGE COUNT 24

16. SUPPLEMENTARY NOTATION

None

17. COSATI CODES			18. SUBJECT TERMS (Continue on reverse if necessary and identify by block number)
FIELD	GROUP	SUB-GROUP	electrooptical devices buried heterostructure
			high-speed diode lasers optical waveguides
			InP optical modulator GaInAsP/InP lasers

19. ABSTRACT (Continue on reverse if necessary and identify by block number)

This report covers work carried out with support of the Rome Air Development Center during the period 1 October 1985 through 30 September 1986.

The small-signal frequency response of small-contact mass-transported buried-heterostructure lasers with minimal parasitic contact pad capacitance has been measured. Initial results show that the highest relaxation frequency of 5 GHz is obtained in long lasers with high optical power.

GaInAsP/InP buried-heterostructure lasers fabricated on p-InP substrates offer considerable advantages in terms of reduced series resistance because of the large-area p-contact. A simple formula has been derived that permits an accurate calculation of the spreading resistance in the p-InP.

20. DISTRIBUTION/AVAILABILITY OF ABSTRACT ☐ UNCLASSIFIED/UNLIMITED ☒ SAME AS RPT. ☐ DTIC USERS	21. ABSTRACT SECURITY CLASSIFICATION Unclassified	
22a. NAME OF RESPONSIBLE INDIVIDUAL Lt. Col. Hugh L. Southall, USAF	22b. TELEPHONE (Include Area Code) (617) 981-2330	22c. OFFICE SYMBOL ESD/TML